



# Design, Modeling and Firmware of a Serial-Chain Multi-Link Direct Drive Flexible Robotic System with Sensor-Augmented Mini-Gripper: Part I

Debanik Roy\*

*Division of Remote Handling and Robotics, Department of Atomic Energy, Bhabha Atomic Research Centre & Homi Bhabha National Institute, India*

\*Corresponding author: Debanik Roy, Division of Remote Handling and Robotics, Bhabha Atomic Research Centre & Homi Bhabha National Institute, Department of Atomic Energy, Mumbai, India

Received: 📅 February 03, 2022

Published: 📅 February 14, 2022

## Abstract

The domain of Flexible Robotics is one of the niche ensembles of present-day robotics research that caters for real-time aspects like rheology, vibration, sensor fusion & non-linear coupled dynamics for control. As some of these features are inherent in a flexible robot, prototyping the same having multiple degrees-of-freedom is highly challenging. This paper reports salient design issues for the firmware of a novel higher-order serial-chain flexible robot and focuses on depth over the hardware development of a prototype multi-link serial-chain direct drive flexible robot fitted with a miniature sensor-instrumented gripper at the free end. The paper also dwells on a new analysis in order to capture the real-time rheology & vibration tuple of the fabricated flexible robot, aided by a novel scheme for sensory layout for its real-time actuation.

**Keywords:** Flexible Robot; Vibration; Rheology; Sensor; Direct-Drive; Hardware; Mini-Gripper; Instrumentation

## Introduction

Design and Hardware manifestation of serial-chain Flexible Robotic Systems (FRS) with multiple slender links is undoubtedly a challenging domain of today's robotics research. Such development attains enhanced significance when we need to attain specific and precise grasp of tiny objects by the end effector / miniature gripper, attached to the terminal link of such multi-link FRS having multiple degrees-of-freedom (d.o.f.). The real-time control over the grasp attracts various interrelated technology-domains, such as rheology (stress-strain paradigms), in-situ vibration, sensor layout & fusion and non-linear coupled dynamics, which comprises the extended envelope of flexible robot research. Characterization and semantics of all these aspects for real-time control of FRS is increasingly become prudent as the system is gaining foothold for a variety of applications in social and medical diagnosis as well as healthcare. It is well-known that despite having a big advantage of very low self-weight the major bottleneck of FRS is its inherent vibration that generally appears at the start of the operation in the form of anything between light undulations to jitter. However, as the operation of the FRS (predominantly the gripping) progresses, this inherent structure-independent randomized vibration gets realized in form of mild to severe trembling of the slender links and/or shaking or twisting of the inter-spaced joints. In

fact, slenderness of the links plays a very important role in self-generation of this trembling, wherein design of the FRS-links & joints become instrumental. The problem gets even complicated when we attempt for multi-link design of the FRS, wherein various kinds of coupled effect & non-linearity crave in. The vibration gets induced to the successive member of the FRS till the end-link as well as the end-effector/gripper. It has been also observed that this self-propagating type of vibration is not time-dependent; in fact, its duration & periodicity can't be correlated with the task-space of the robotic system. The measure of this run-time vibration can be done in two ways, namely: modal frequency & eigen vector. Thus, real-time assessment of vibration signature in FRS is a pre-requisite for establishing a reliable control system for any real-life application.

The vibration models in FRS, used hitherto, have been found to be somewhat inappropriate for real-time monitoring & control of the payload, i.e., the object to be gripped at the end-of-arm tooling. We will report a new approach of modeling this inherent vibration using geometrical facets of the FRS in this paper. The mechanical hardware of the prototype serial-chain direct-drive multi-d.o.f. FRS will be described in detail, based on this vibration analysis-based design model. It is important to note that in all practical applications, this vibration signature gets assessed in real-time through multiple

force sensors, spread over the links & joints of FRS. However, the dynamics effect due to various geometrical configurations of the FRS-links as well as link-wise (zonal) distribution of these sensors in the FRS was largely unattended. A comprehensive look towards this zonal effect has been presented in this paper: Control issues of FRS have gained research attention over the last few decades, which deal with novel techniques of control of system dynamics in real-time [1]. While perturbation method was tried for fine-tuning FRS-controller [2], direct real-time feedback from strain gauges was experimented too [3]. It is true that a robust dynamic model becomes very effective in understanding the behavior of FRS in real-time and the same becomes crucial for a multi-link FRS [4,5]. Felio et al attempted the control issue of a three degrees-of-freedom FRS using the methodology of inverse dynamics in contrast to strain gauge-based control [6,7]. The fuzzy learning-based approach for control of FRS was also reported by Moudgal et al. [8]. Specific metrics related to reduction of system vibration of a robotic gadget were attributed by Singer & Seering [9]. Various techniques for vibration attenuation & control in FRS have been reported hitherto, such as sliding mode theory [10], adaptive resonant control [11], online frequency & damping estimation [12] & integral resonant control [13]. Dynamic model & simulation of FRS based on spring and rigid bodies was established too [14]. It is important to comment here that laboratory-based experimentation on the control semantics of single-link flexible robot gained substantial leverage over the years. These flexible arms have served as robust testbed for various new control strategies like load-adaptive control (using end-of-arm mass) [15], end-point control [16] and acceleration-feedback control [17]. However, modeling of the multi-link FRS using compliant sub-assemblies, such as spring-dashpot-damper, remains an open research domain till date.

It may be stated that experimental mode of modeling & control of in-situ vibration of FRS needs a strong encapsulation of sensor data structure, data assimilation and finally, statistical analysis of the grasp by the FRS-gripper. Stochastic modeling & novel hypothesis testing-based decision theory for robotic grasp have been delineated in [18]. The real-time application of the developed hypothesis testing-based decision thresholding for dissimilar sensor-cells in a robotic gripper sensor has been reported [19]. Based on these earlier attainments, we will propose here a new theology on deformation & deflection for the real-time analysis of vibration data of FRS. Chronological survey on FRS research reveals that nearly all studies worldwide till date are concentrated on various experiments on the control synthesis of single-arm FRS with or without end-mass. Kinematic & dynamic effect of end-of-arm tooling and/or gripper in such FRS was also not addressed hitherto. However, both rheology & vibration characteristics of FRS will drastically alter as soon as jointed structure is in place, i.e., multi-link multi-jointed FRS with a miniaturized gripper fitted at the open end. We have investigated such scenarios of control dynamics for a multi-degrees-of-freedom FRS fitted with mini-gripper [20], postulating spring-dashpot-based model (for

vibration signature) and strain gauge-induced model (for dynamic strain signature). Firmware of a multi-link serial-chain FRS using flexible shafts for drive motion of the joints have been developed by the author's group [21,22].

The paper has been organized in six sections. An overview of the possible design variations and analysis mechanical sub-assemblies of the serial-chain FRS are presented in the next section. Representative layout for sensor augmentation as well as synthesis of in-situ vibration and control dynamics model of the developed FRS has been addressed in section 3. The mechanical hardware of the fabricated FRS is reported in section 4. Section 5 addresses the paradigms of the control system algorithm & development of the controller of the prototype FRS and finally, section 6 concludes the paper.

### Serial-Chain Flexible Robotic Systems: Design & Mechanical Sub-Assembly Analysis

Two major variants of the link-design of serial-chain FRS have got standardized in recent past. These are: a) 'rod' type link & b) 'plate' type link. While 'rod' type FRS-link will have circular cross-section, the 'plate' type FRS will have links in the form of thin plates, either of square or rectangular cross-section. Based on these two fundamental configurations of the FRS-link, auxiliary design-metrics have been arrived at so as to make the ensemble design foolproof. A considerable amount of research effort was put forward during the first phase towards investigating the in-situ deflection / vibration paradigms of single-link FRS without an end-mass. Subsequently, design metrics were established for single-link FRS with an end-mass of finite volume. However, this end-mass is no way, comparable to the dynamics of the end-of-arm tooling and/or gripper, especially in the scenario of vibration-based studies on FRS. The other crucial design paradigm that was often missed or overlooked by the researchers is the tapering of the FRS-link(s). A tapered cross-section FRS-link will naturally be a wise choice for the design for manufacturing, as it will help reducing the ensemble tare-weight of the system. The conceptual design of the multi-d.o.f. serial-chain FRS does depend on the design & modeling of the single-link FRS to a large extent.

As seen in Figure 1, we have introduced the concept of 'Datum', which is a fundamental metric of the analytical modeling of the FRS. We come across two types of Datum in any serial-chain FRS, viz. a)  $D_R$ : the real or actual datum of the FRS, which is essentially the extension of the FRS-base in horizontal plane of reference and b)  $D_p$ : the pseudo or virtual datum of the FRS, which is nothing but an imaginary plane passing over the span of the FRS-link. A solid spherical end-mass is used for the purpose of modeling the run-time deflection of the FRS (refer 'F' of Figure 1); however, the real-time dynamics of the end-of-arm tooling will alter considerably whenever a miniature gripper will be used instead. It is crucial to note here the vibration and/or rheological features of the FRS do alter under two situations of end-of-arm attachment, viz. end-/

tip-mass vis-à-vis a mini-gripper (at the distal link of the FRS). Figure 2 schematically illustrates the two major design ensembles of serial-chain FRS, namely, [a] Rod-type link & [b] Plate-type link. In both types, the schematic of the link has been conceptualized as an enclosed perimeter in 2D having four distinct vertices, namely, {A, A', B, B'}. The nomenclature of the said planar perimeter can be coined as: [AA'B'B], using counterclockwise norm. It is prudent to

designate Cartesian co-ordinates of the endpoints of the central axis of the FRS-link. Accordingly,  $(x_i, y_i)^c$  and  $(x_j, y_j)^c$  symbolize the planar Cartesian Co-ordinates of the left-hand-side and the right-hand-side point of the Central Axis of FRS-link respectively. In a similar logic, we can assign co-ordinates of the four vertices of the FRS-link as: [A:  $(x_i, y_i)$ ; B:  $(x_{i+k}, y_{i+k})$ ; A':  $(x_{j+k}, y_{j+k})$ ; B':  $(x_{j+k}, y_{j+k})$ ], where 'k' is the planar width of the FRS-link.

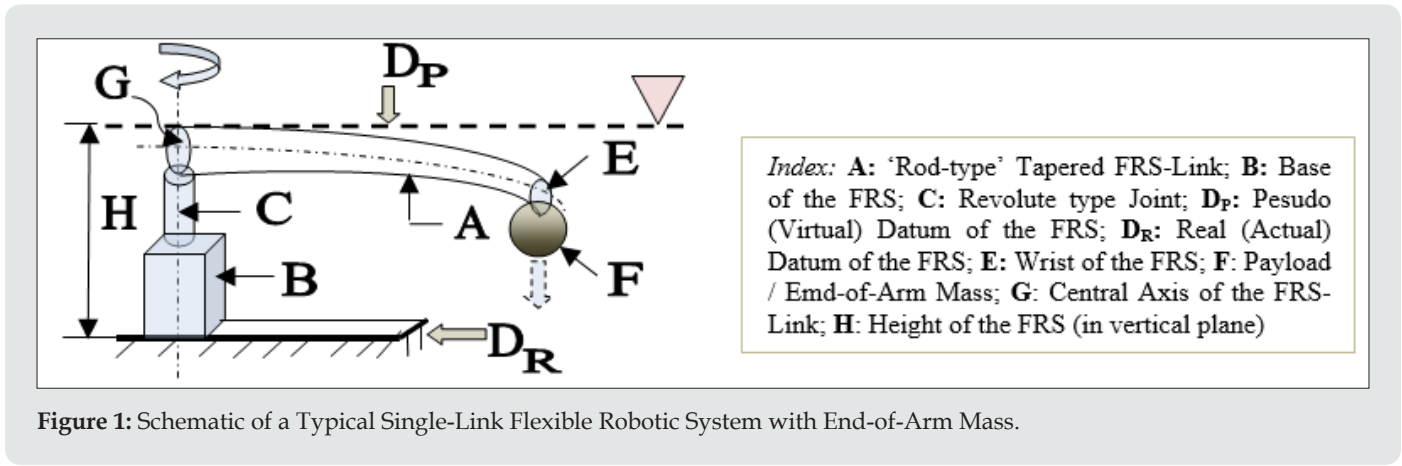


Figure 1: Schematic of a Typical Single-Link Flexible Robotic System with End-of-Arm Mass.

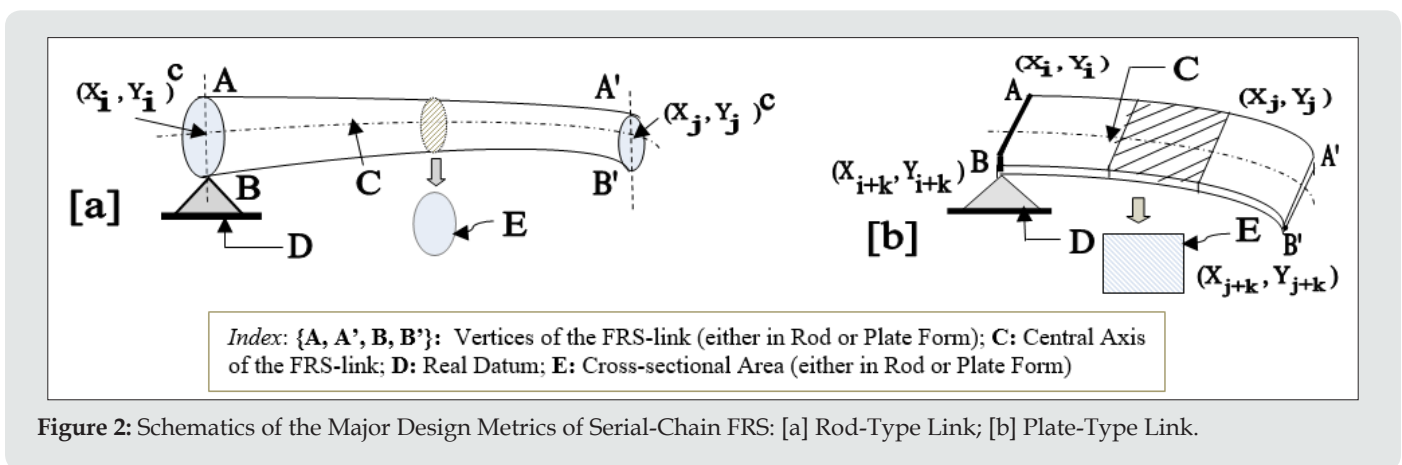


Figure 2: Schematics of the Major Design Metrics of Serial-Chain FRS: [a] Rod-Type Link; [b] Plate-Type Link.

It is important to note at this juncture that nature as well as physical size of the cross-section of FRS-link(s) play significant role in the ensemble deflection of the system in real-time. This deflection can be modeled as curvilinear elongation once steady state is achieved post-vibration. Along with as-manufactured dimension of the cross-section, the span of the FRS-link, either in totality or partial, becomes instrumental in culmination of the signature of the curvilinear deflection. Figure 3 schematically illustrates the proposition of real-time deflection of a rod-type FRS-link and its geometrical measure. The design characteristic of a FRS demands super-slender structure so as to register in-situ vibration / trembling of its links. However, it is important that steady state of this vibration reaches very quickly. The measurement / estimation of the actual curvilinear deflection value can be carried out after the system attains sufficient stability. In this context, the actual

estimation of deflection will be made for  $dz$ , using the geometry of the  $\Delta OAA'$  (with numerical value of  $dx$  known a-priori).

The other salient design feature of a typical FRS is the non-uniformity of the cross-section, namely, gradual tapering. Tapered cross-section of the FRS-link is always preferred from the viewpoint of design as it calls for reduction of volume and thereby, mass of the link. Naturally, FRS with lower tare-weight will always be an ideal choice so far as research on flexibility and/or compliance is concerned, notwithstanding the practical difficulty to control the same in real-time (i.e., with enhanced slenderness of the cross-section). In fact, design of tapered cross-section for the FRS-link is well-recognized in the research community and, that's the reason we have also addressed the fundamentals of FRS-design with tapering of the link till now (refer Figures 1,2a, &3). Although

design of tapered cross-section is foolproof, its manufacturability is not straight-forward. As on date, there is no well-established manufacturing method to generate tapering in non-metallic materials under mass production. Since use of non-metallic

material is usually preferred for the fabrication of multi-d.o.f. FRS because of less tare-weight, manufacturing tapered cross-section for such FRS-link(s) remains troublesome.

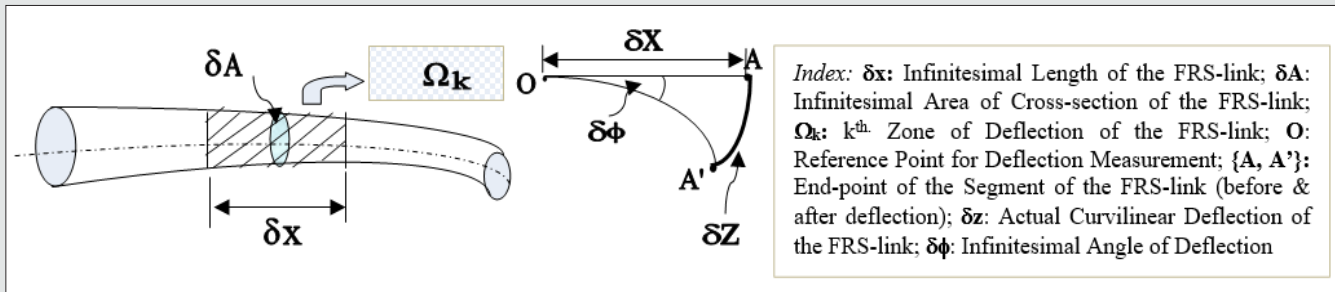


**Figure 3:** Schematic of the Real-time Deflection of the FRS-link after Attainment of Steady State of Vibration.

Nonetheless, three fundamental categories of tapering are possible to be fabricated from the perspective of design, viz. a] straight taper (angle of taper remains constant); b] uni-curve taper (angle of taper varies in proportion to the curvature) & c] bi-curve taper (angle of curvature alters twice). Out of these, we will illustrate the straight tapered cross-section of the FRS-link with its engineering as well as analytical perspective in this paper. Figure 4 shows two types of possible cross-section of the FRS-link with straight taper, namely, decreasing-type and increasing-type (from left-hand-side to right-hand-side) for a single-link FRS-arm. The diagrammatic nomenclature has been made generalized, with respect to  $i^{th}$ . link of the FRS ( $\forall i=1,2,3,\dots,n$ ). It may be noted here that the numerical measure of  $D_i$  will be dependent on the exact shape of the cross-section (circular, rectangular, square etc.), apart from the dimensions. The angle of inclination,  $\theta$  is the measure of the flexibility or compliance of the FRS-link at various section-

planes. Cartesian co-ordinates are established at both ends of the  $i^{th}$ . FRS-link, viz. at two joint-locations ( $J_{i-1}$  &  $J_i$ ) within an inner span ( $L_i$ ). As evident from the schematic of Figure 4, the common features of the design with tapered FRS-link are: i] variation of link cross-section at different transverse sections, e.g. section  $[A-A']_p$  and ii] variation in link inclination at different locations of the link, e.g.  $\{c\}_i^k$ , as 'instantaneous measure of flexibility'. Mathematically, for N-link FRS we can state these two propositions using proportionality constants  $\xi$  &  $\lambda$  :

$$[D_i]^p = \xi \cdot \langle L_{A-A'} \rangle_p \quad \forall i \in N, p \subset (J_{i-1}, J_i) \quad (1)$$

and

$$\{\theta\}_i^k = \lambda \cdot \langle L_c \rangle_k \quad \forall i \in N, k \subset (J_{i-1}, J_i) \quad (2)$$

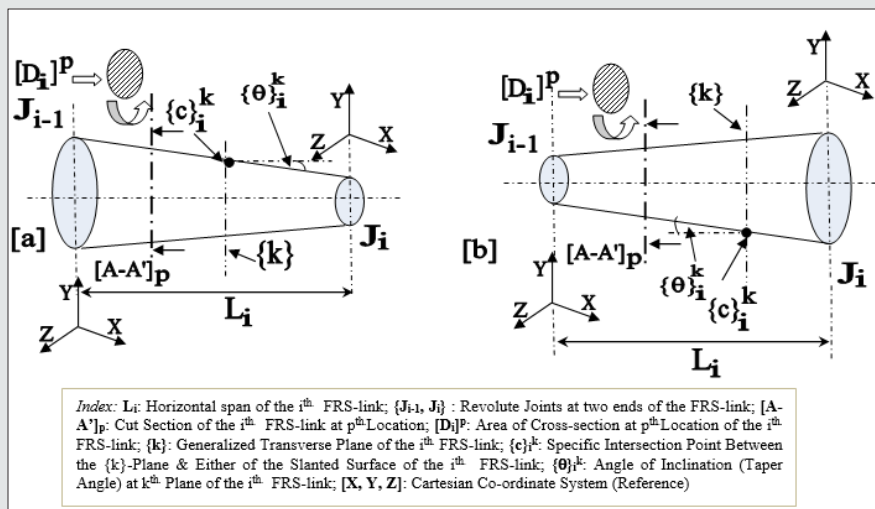


**Figure 4:** Schematic & Analytical Paradigm of Straight Taper of FRS-Link with Cross-sections: [a] Decreasing; [b] Increasing.

Also, by geometric proposition, we can get an estimate of the instantaneous angle of taper as:

$$\tan \theta_i = \frac{(D_R - D_r)}{2L_i} \forall i \in N \tag{3}$$

where,  $D_R$  &  $D_r$  signifies the larger & smaller diameters of the FRS-link respectively.

We have adopted direct-drive approach in the present hardware that calls for integration of miniature servomotors at the joints. This design is moderately backlash-free because of the closeness between the motor-shaft & joint-shaft. This proximity makes the entire joint sub-assembly robust so far, the control of the joint in real-time is concerned. However, direct-drive technology in FRS suffers from poor vibration control. In fact, trembling or in-situ vibration becomes more prominent in case of direct-drive FRS, due to the addition of weight of the servomotors at the link-joint interface that causes overall enhancement of the tare-weight. With this perspective of pros & cons of the direct-drive approach,

we get a wider band of research paradigms to tackle in the case of our prototype FRS. Figure 5 presents an ensemble schematic of the prototype compact-volume direct-drive type serial-chain FRS, having three links & three revolute joints. In order to add generality, legends of Figure 5 have been adopted so as to cater for a multi-link multi-joint serial-chain FRS as well. For example, overall span in horizontal plane of a n-link FRS is indexed as  $\Sigma L_i$ , where link-lengths are denoted by  $L_i, \forall i = 1,2,3,\dots,n$ . Likewise, the revolute joint-ensemble and servomot-ensemble are indexed as  $\{J_i, J_{i+1}, J_{i+2}, \dots, J_{i+n-1}\}$  and  $\{M_i, M_{i+1}, \dots, M_{i+n-1}\}, \forall i = 1,2,3,\dots,n$ . The drives for all three joints of the FRS are 'direct'. As illustrated in Figure 5, the jaws of the mini gripper are actuated through a dedicated servomotor,  $M_g$ , located at the backside of the gripper baseplate. The base mechanism of the prototype FRS is composed of two sub-assemblies, viz, housing, B1 & tripod-type support stand, B2. The hardware manifestation of  $\{B1, B2\}$  tuple signifies the vertical clearance of the FRS over the horizontal plane in manoeuvring through its workspace.

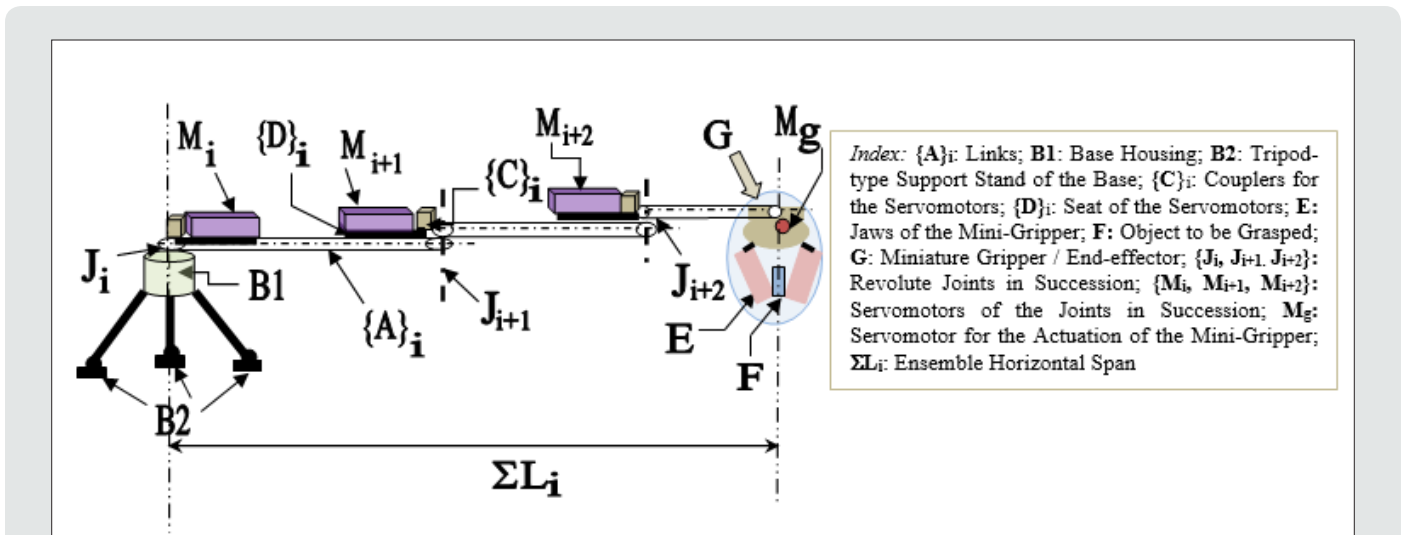


Figure 5: Ensemble Schematic of the Prototype Serial-Chain Direct-Drive FRS.

One important paradigm of a serial-chain FRS is related to the optimal joint design. Our prototype serial-chain FRS being planar, all joints are ideally conceived as revolute type, undergoing coplanar motions. The joints have a rotating shaft, miniature ball bearings, end-covers, housing and a special element at selected joint(s), viz. cross-flexures. The design of the joint is correlated to the design of links too as the end-fittings of the link(s) will be an extended part of the joint assembly. This link-joint mating zone is very significant in the prototype FRS, unlike usual serial-chain robotic manipulator. The schematics of the revolute joint assembly of the prototype serial-chain FRS (with and without cross-flexures) are shown in Figures 6a & 6b respectively. It may be mentioned here that the set of four cross-flexures per ball bearing, namely, CF1

to CF4, as shown in Figure 6b plays a significant role is adjusting the lateral positional shiftment of the revolute joint, if required. These cross-flexures designed & manufactured indigenously are fitted by the side of the ball bearing outer cage in such a fashion so as to provide requisite play to the ball bearings during the rotational motion. The cross-flexures, have been designed as small wedges, in the shape of right-angled triangle. A fresh set of four cross-flexures will be fitted in the ball bearings at lower rung as well (not shown in Figure 6b). Cross-flexures have been provided in last two revolute joints of the prototype FRS, in order to compensate for the in-plane vibration of the ensemble hardware. The base joint ( $J_1$  of Figure 5) is fitted with bearing sets as per schematic of Figure 6a.

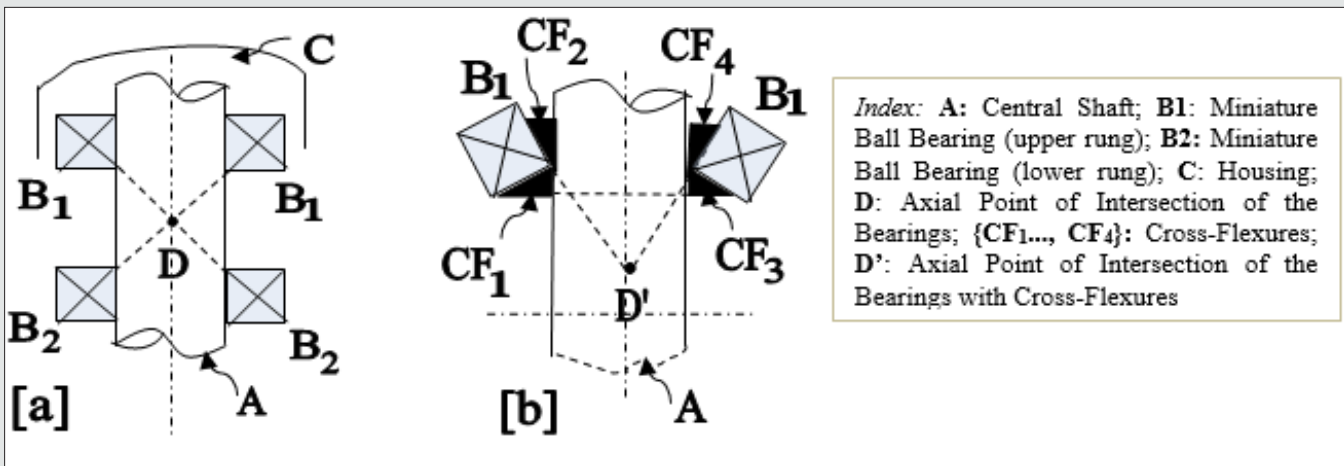


Figure 6: Schematics of the Revolute Joint Assembly of the Prototype FRS: [a] Without Cross-Flexures; [b] With Cross-Flexures.

The prototype serial-chain direct-drive FRS is manufactured with four sub-assemblies, viz. a) Base; b) Link & Joints; c) Mini-gripper & d) Drive system & controller. The novelty of the base sub-assembly [(B1, B2) of Figure 5] lies with its interconnection with the first link (A<sub>1</sub> of Figure 5) and system controller. The prototype FRS works at a pre-assigned vertical span and attains its planar disposition with respect to the movement of the end-effector (G of Figure 5). The link & joint sub-assembly is the backbone of the prototype as it maintains the synergy between the link, actuating

joint & driving servomotor. It is to be noted that we have incorporated only the servomotor, responsible for the actuation of the specific joint in the link assembly. The present FRS-prototype has a niche in mini-gripper sub-assembly too. Besides size miniaturization, it has a unique design for the jaws. As seen in Figure 5, both jaws of the mini gripper are flat plate type and are being driven by spur gears & actuated through a customized linkage on either side (fitted between the base plate & the jaw).

## Synthesis Of Vibration and Modeling of the Control Dynamics of the Prototype Flexible Robot

### Synthesis of In-situ Vibration

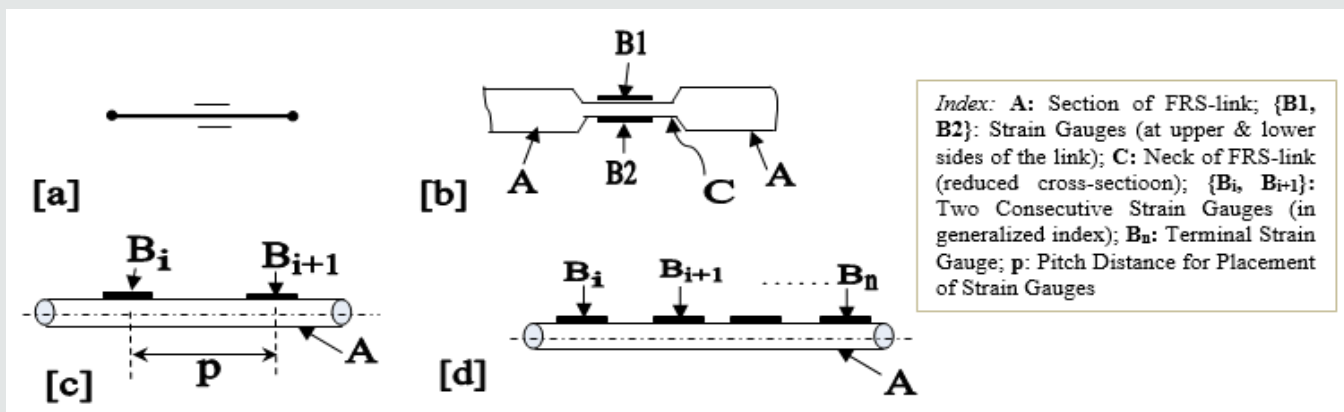


Figure 7: Representative Layout of Strain Gauges in FRS: [a] Basic Line Sketch; [b] Fixation Metric; [c] Pitching; [d] Generalized Form.

The ensemble motion of any link of a flexible robot in real-time is a conglomeration of two entities, namely: a) rigid motion (similar to Euler formulation of rigid body dynamics) & b) elastic motion (description of the deformation state). While the rigid motion is characterized by the rheology of the FRS, e.g., strain

vectors of the links / joints, the elastic motion serves as the source for the inherent vibration of the system. However, it is difficult to determine these two entities experimentally, as the conjugate effect of the deflection of the FRS-link gets subsumed into one another. The only experimental method that can be adopted to measure

the conjugate strain of the FRS-link is through the excitation of multiple strain gauges, placed over the external surface of the link(s). As a matter of fact, the paradigm of in-situ vibration of FRS-link can be symbolized as the real-time deflection of a cantilever beam, having relatively larger deflection potential at the 'free' end. Cantilever-type FRS-members do possess easy potential for affixing sensing element(s) as well as better relief at the non-fixed end. Figure 7 schematically illustrates the experimental preparation of interfacing multiple strain gauges at pre-assigned locations on the FRS-link(s). The location of placement of strain gauges have been marked by '=' symbol in Figure 7a, while legends are used for the same in Figures 7b-7d.

The material-specific deformation of FRS-member at any time-instant is a combined effect of natural frequency of vibration and total strain produced inside the said member. The principal axis of such deformation and/or deflection is curvilinear. The multi-modal nature of the in-situ vibration of the FRS can be modeled optimally through spring-damper-dashpot design scheme of the FRS-link. Figure 8 schematically shows our novel model for the study of the in-situ vibration of the FRS. This conjugate spring-damper-dashpot model is the key to the assessment of the modal frequencies (1st. to Nth. mode). The spring-damper system is self-compensated and the resultant vibration, generated thereof, will be the optimal amount

required for stimulating the FRS-ensemble. Our model for the conjugate spring-dashpot system depends primarily on the extent of in-situ vibration that is expected out of the external excitation of the prototype FRS. The number of such conjugate systems, i.e., D1, D2, ..., Dp will be determined by the simulated values of the natural frequency of vibration. The requisite vibration study was carried out via Finite Element Analysis. It is important to note that an efficient dynamic model of FRS will be able to characterize deformation & deflection of the FRS-members in real-time. At times, these two entities are quite inseparable, and we need to rely on trial-run of the hardware only. Nonetheless, we can comment that while initial trembling of the FRS is solely due to the basic natural frequency of vibration, its gradual increment during the course of real-life operation is due to the second as well as third modal frequencies. The FRS becomes more vibrant and sometimes, out-of-bound at fourth & fifth modal frequencies because of the progressive gradual increment of the natural frequency. The system is expected to imbibe higher level of internal stress, especially at the joints and link-joint interfaces during the next higher modes of vibration, i.e., sixth, seventh or eighth modal frequencies. The control system of the FRS may fail completely at ninth & tenth modal frequencies unless suitable harnessing is adhered. These two higher modes are truly undesirable for any working-level prototype of FRS.

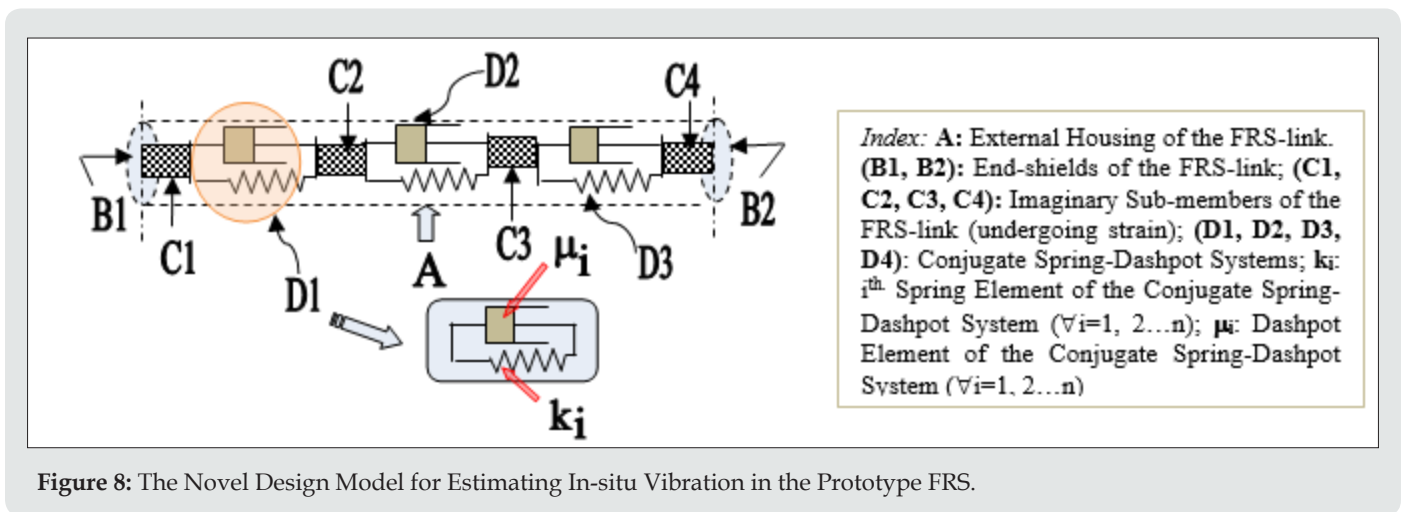


Figure 8: The Novel Design Model for Estimating In-situ Vibration in the Prototype FRS.

### Modeling of Control Dynamics

The nucleus of FRS-dynamics is the built-in vibration and its incarnations, i.e., higher-order modal frequencies. The inherent vibration of the flexible robot is directly proportional to the number of degrees-of-freedom of the FRS. On the other hand, the dynamic strain vector (  $\epsilon_i, \forall i = 1,2,3,\dots,k$ : where 'k' is the link-number of FRS) is evaluated from structural analysis of the FRS. Thus, the paradigm of control dynamics of FRS in real-time essentially involves investigation of strain vis-à-vis vibration tuple. In case of 'direct-to-joint-drive' serial-chain FRS, the instantaneous real-time displacement will be prudent in the links in the form of 'deflection' and micro-twist at the link-joint interface areas. We will postulate

the fundamental equation of control dynamics of the serial-chain FRS, using measurable parameters. We will treat the serial-chain FRS as open-end cantilever structure, thereby imbibing spring-effects at the links & joints. The ensemble deformation at the FRS-joints will be accounted as friction torque while stiffness will be estimated through viscous damping of the joints. The following equation is arrived at in support of the real-time dynamics of the FRS:

$$[M_i] \frac{d^2\theta}{dt^2} + \{B_i\} \frac{d\theta}{dt} + [K_p + K_v](\theta - \delta) + (\tau_i), \forall i \in N, p \in (J_{i-1}, J_i) \dots \dots (4)$$

where, i: link number; p: joint index; J<sub>i-1</sub> & J<sub>i</sub>: Consecutive revolute joints; θ: Rotation of the link; M: Desired moment of inertia matrix

of the link;  $B$ : Desired viscous damping (friction) coefficient;  $K_p$ : Desired stiffness of the joint;  $K_l$ : Desired stiffness of the link;  $\delta_p$ : Initial angular position of the link and/or joint;  $\tau_f$ : Frictional torque;  $\tau_l$ : Load torque;  $N$ : Real numbers. It may be observed that the proposed dynamic model of the FRS is essentially torque-induced material equation, wherein selection of appropriate material for the links as well as the joints is very crucial. The terms of the dynamic model equation include vectors of angular velocity & angular acceleration that need to be determined through real-time experiments.

### Mechanical Hardware of the Fabricated Flexible Robotic System

Rheology-based simulation of different types of serial-chain FRS has made a strong foundation for the hardware manifestation of the final prototype system. We have successfully developed the working prototype of the serial-chain FRS, having revolute joint-actuated three uniform cross-section links of unequal length and one miniaturized gripper at the distal end. As explained earlier, all revolute joints are being actuated through D.C. servomotors (Make: Faulhaber™), integrated with gearbox & encoder. The flexible robot is equipped with several limit switches for each servomotor in both directions so as to invoke precautionary measure for overrun of the rotary motions. We will describe the hardware of the FRS in the order of its sub-assemblies, as per the layout shown in Figure 5.

#### Fitment of the First Link & Base Sub-Assembly

The fitment of the first link with the base of the FRS is very crucial as it has to cater for its own rotary motion as well as sliding motion of the tripod system. Figure 9a shows the photographic view of the fitment, wherein the first link is assembled with a polymer-box protective housing encapsule that contains a 12V D.C. power supply for effective insulation. This housing box also contains Faulhaber™ motor controller, which is meant for running the first joint motor ( $M_1$  servomotor: refer Figure 5) and make-shift ball screw for the fixation of the tripod & base ( $B1$  &  $B2$ : refer Figure

5). A closer view of the link sub-assembly is presented in Figure 9b, highlighting the mounting of the first link over the housing-box. This link sub-assembly can be rotated in a range of  $0^\circ$  to  $270^\circ$  by the servomotor, placed inside the encapsule. The top-box also has 25 pin connectors that are connected to various sensors (used in the prototype) as well as servomotors for the rotation of link 2, link 3 & mini-gripper. It is needless to state here that wiring diagram & instrumentation thereof for this sub-assembly is tedious and we used standard colour coding of the wires for easy trackability inside the FRS-ensemble. It is important to note that these 25 pin connectors are trademarked and cannot be used as RS232C and/or parallel port connection of computer in any way. The first link of the prototype FRS is 800 mm long and it is fitted with 10 strain gages over its periphery (i.e.,  $n=10$ , as per Figure 7d). This is, in fact, the maximum number of strain gauges in comparison to the other two links as the first link is bearing the maximum working stress. The fitment of the recirculating ball screw, amidst the top-box & cable-wiring, is shown in Figure 9c, which is the in-process procedure for the base sub-assembly. It is important to state here that the sub-assemblies for the first three links have got some commonalities from the viewpoint of fabrication. As observed in Figures 9a & 9b, fitment of the first link was made with the help of a moveable support (refer 'C') and a working platform (refer 'D'), made of teflon. These accessories are very crucial because of the slenderness of the first link. Once the fitment of the first link with the polymer-box was done, rest of the assembly was carried out on 'D'. (Refer Figure 9b). The sub-assemblies for second & third link were made with the help of this working platform only. The next crucial sub-assembly was that of the tripod (and temporarily recirculating ball screw), which was supported by the metaling stand, tripod support lever & tripod fixing jig (refer 'E', 'F' & 'G' in Figure 9b). The mounting of the ball screw (refer 'I' in Figure 9c) is properly aligned with the help of these three members, with subtle handling of the cable-wirings & strain gauge-fixation wires. We will revisit the ensemble of ball screw assembly while describing the tripod assembly.

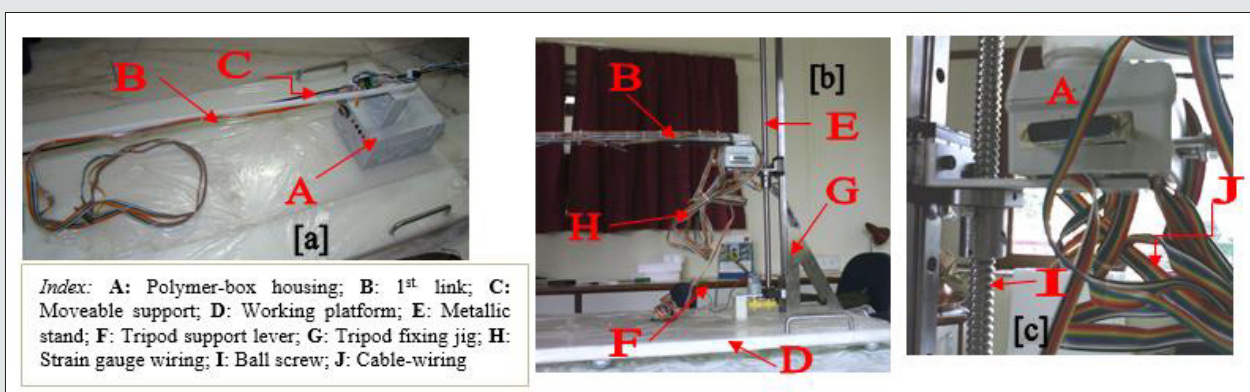


Figure 9: Photographic View of the Fabricated FRS: [a] Fitment of 1st. Link; [b] Sub-assembly of 1st. Link & [c] Fitment of Ball Screw.

## Second & Third Link Sub-assembly

In contrast to the first link, the design for the subsequent links of the prototype FRS has been made with reduced lengths but without altering the uniformity in cross-section. The second link is half of the size of the first one, i.e., the length of the second link has been kept as 400 mm. As effect of in-situ vibration is ideally predominate in the first link, we have fitted only one strain gauge over the surface of the second link. The third link is the shortest; its length is 200 mm. only. No strain gauge is fitted on the third link as the vibrational effect of it is being subsumed in that of the mini gripper, attached at the end of the third link. Both second & third links are actuated by Faulhaber™ make D.C. servomotors.

## Joint Sub-assemblies

The prototype FRS has got two revolute joint assemblies, which are identical as well as interchangeable. The first joint is placed

between the first & second link (link 1 & link 2) while the second joint is positioned in-between second & third link (link 2 & link 3). The crux of the joint design is the base of the joint, manufactured from fibreglass, i.e., Carbon Fibre Reinforced Plastic (CFRP). This base is fixed with the Faulhaber™-make servomotor on one side and teflon-made rotating pad on the other side. The motor-shaft protrudes through the base and is being connected to a small spur gear pair. While the smaller gear is mounted on the motor-shaft the bigger one is attached to the rotating pad. These two gears must not mesh with each other, and the gear-train should be disengaged prior to the re-fixing of the joint assembly. Figure 10a shows the photographic view of a typical revolute joint used in the prototype, along with the link and the corresponding motor controller. The disposition of the second link is illustrated in Figure 10b and that of the third link (Alongwith the gripper) is shown in Figure 10c.

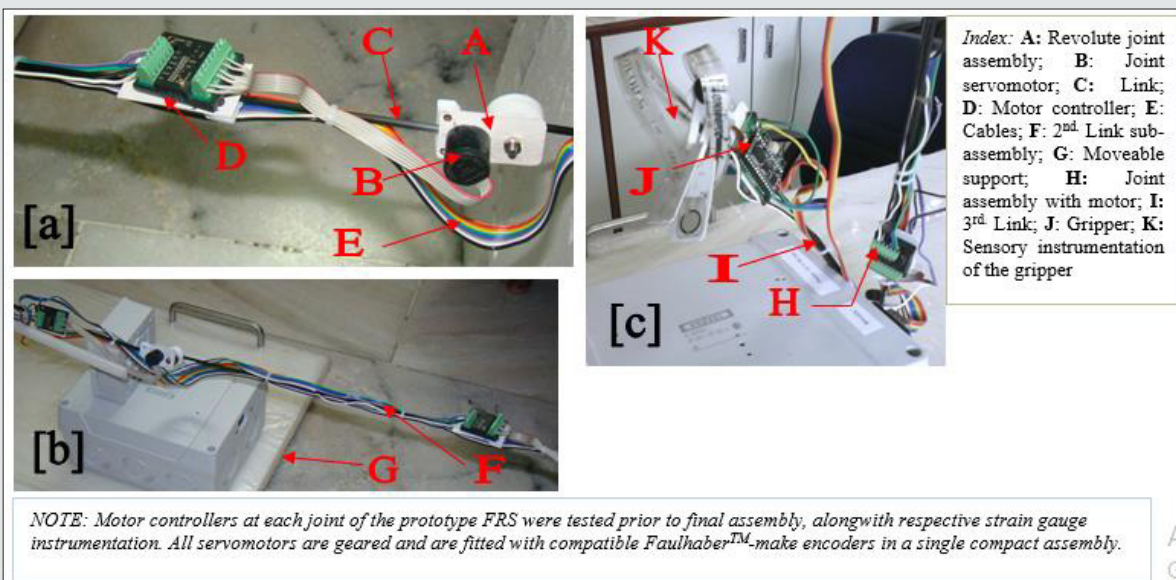


**Figure 10:** Photographic View of the Fabricated FRS: [a] Revolute Joint; [b] Sub-assembly of 2nd. Link & [c] Disposition of 3rd. Link.

## Gripper Sub-assembly

The essence of the indigenous design of the gripper is its lightweight and compact structural ensemble, which is largely attributed to the use of non-metallic materials for the fabrication. The gripper-motor (Faulhaber™-make) is mounted on a fiberglass base with its output shaft fitted with a tiny spur gear. The motion of the gripper-jaws is governed by a compact spur gear-train and is being transmitted to the jaw-plates through a pair of slender linkage. The tare weight of the gripper is 100 gm (approx.), fitted with the motor. Being a very light-weighted entity, the motor of the gripper is operated at a significantly low electric current rating. This necessitated mounting of the motor-controller in close vicinity to the gripper body. The spur gear pair was fabricated in close manufacturing tolerances so as to minimize the spatial layout.

The pinion gear is mounted on the output-shaft of the servomotor that in turn drives the larger gear in unison. The uniqueness of the design is centered over the jaw plate ('finger'); unlike other typical designs of robotic grippers, we have fixed each jaw plate separately to the gears by means of a linkage. Figure 11a shows the photographic view of this mini-gripper (frontal side), as fabricated indigenously. It may be noted that all the sub-assemblies of this gripper were carried out manually, using hand precision. The disposition of the mini-gripper from the side is illustrated in Figure 11b, exposing the integration of the motor-controller & allied sensory instrumentation. Because of this novel design, it is easier to pin-point the motion of the fingers in close association with the motion of the gear-pair. As the gears rotate in opposite directions, the fingers also perform the sequence of opening & closing operation, maintaining a curvilinear path.

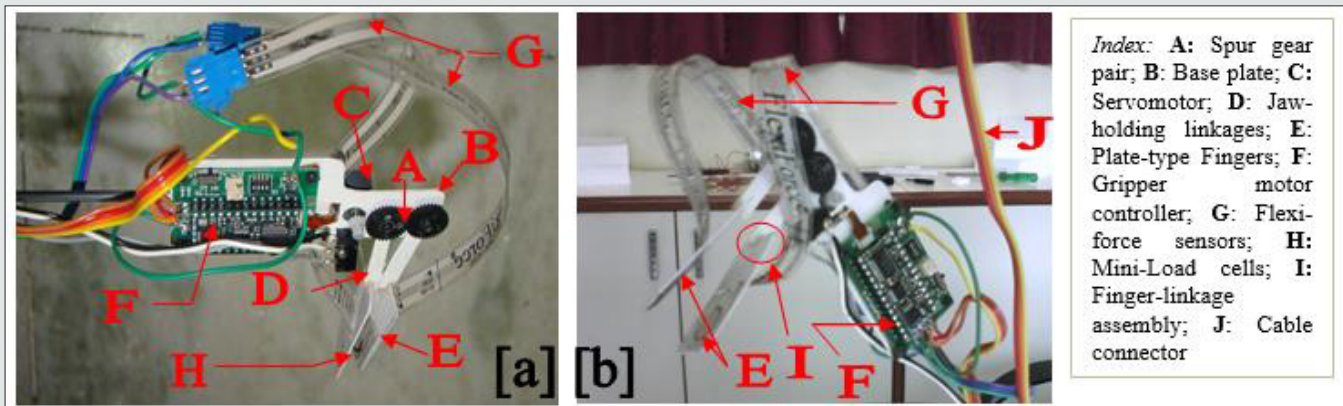


Figure 11: Photographic View of the Fabricated Mini-Gripper of the Prototype FRS: [a] Frontal View; [b] Side View.

A pair of tiny load cell (Entran™-make) is mounted on the fingers at the tip. The load cells are ultra-sensitivitive & precis, which can be tested even with finger-touch. As the flexible robot is intended for grasping & picking of very light-weighed objects, such as paper, medicine pill, plastic spoon etc. the load cells are perfect for detection & evaluation of gripping force of very small order. The load cells are connected to colour-coded wires with special BERG-type connectors. The entire assembly was extremely delicate as the prime most attention was to keep the tare weight of the gripper minimum. It is to be noted that all small gears, used in this mini gripper, are custom-made as the design could not have been

compromised for size & weight limitations. We selected acetal™ as the material of these gerars after several iterations to test the functionality & durability. All acetal™-made gears are impervious to water and are light-weight too. However, these gears may be reactive to organic solvents that may be avoided during operation. The ensemble fabrication and assembly of the prototype FRS was undertaken in four major sub-assemblies, as described above. The Tripod sub-assembly was made with three small rollers, and it was fitted to the base sub-assembly. Figure 12 shows the photographic view of the final assembly of the fabricated prototype of the three-link flexible robot.

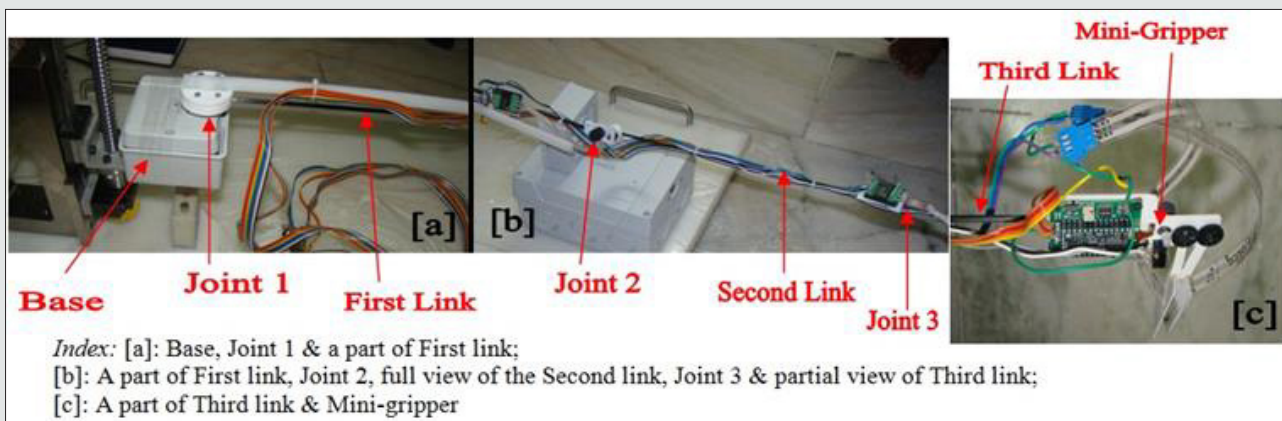


Figure 12: Photographic View of the Final Assembly of the Fabricated FRS.

### Control Logic & System Controller of The Flexible Robot: Highlights

The backbone of the control system algorithm of the fabricated flexible robot is Proportional-Integral-Derivative (PID) control, augmented by current-based cut-offs and electronic limit switches. On the other hand, the controller of the flexible robot is a retrofit of Faulhaber™-make Motion Controllers (MCBL & MCDC series). The

developed flexible robotic system gets operated through 12V D.C. source. A power supply unit was made, consisting of two identical 12V D.C. supplies inside the housing. Either of these power supplies can be used to charge a 70 AH battery. The power requirement design of the flexible robot has been made in such a manner so as to match for battery-based functioning as well, in cases of emergency. The controller is equipped with easy provision for disengagement of power supply unit as & when battery-based activation of the FRS is

invoked. The controller of the prototype FRS is designed & fabricated for indoor use, having relative humidity of the environment varying from 10% to 80%. As Faulhaber™-make Motion Controllers are sensitive to heat, it is advisable to avoid direct sunlight & dust during operation of the prototype, irrespective of its working environment. The prototype FRS is equipped with limit switches for overrun protection of each servomotor in both directions. These limit switches have been interfaced with the system controller in a way so that those get triggered at the extreme ends of the links and gripper. The binary output of the limit switch is incorporated in the control program so that the corresponding motor stops as & when the switch is triggered. The individual motor controllers are interfaced with RS232C port of the computer, which makes the overall system user-friendly from operational standpoint. Although the model of the Faulhaber™ motor controllers are not all same, but the basic logic of operation is identical. All servomotors of the FRS as well as the tripod motor are controlled by Faulhaber™-Motion Manager software, which has user-selectable drop-down menus for the desired control parameter.

## Conclusions

All four sub-assemblies of the prototype FRS were functional building blocks for the ensemble, and we could testify it too. The piece-meal testing of the joint controller, sensory instrumentation & gripper operation gave an edge over the final assembly of the FRS towards full proofing the same. Besides manufacturing, a new model for in-situ vibration signature of a multi-link flexible robotic system using spring-dashpot-damper and strain gauges is also reported. The present research builds up an optimal foundation for analyzing inherent vibration of flexible robots and its performance in gripping small payload in real-time, using scientifically ascertained locations of fixing strain gauges over the FRS-links. The indigenous hardware of the prototype serial-chain three-link flexible robotic system will be instrumental in creating novel designs for similar such FRS with sensory instrumentation.

## Acknowledgement

Author acknowledges the help rendered by Shri Uday Phalnikar, Ex-BARC & Prolific Systems & Technologies Pvt. Ltd., Thane, India in assisting the hand-made sub-assemblies of the links & gripper of the prototype FRS. Fabrication-related assistance provided by the engineers of M/s Devendra Fabricators, Nashik, Maharashtra is duly acknowledged.

## References

1. M Benosman, G Vey (2004) Control of Flexible Manipulators: A Survey. *Robotica* 22: 533-545.
2. AR Fraser, RW Daniel (1991) Perturbation Techniques for Flexible Manipulators. Norwell MA Kluwer.
3. ZH Luo (1993) Direct Strain Feedback Control of a Flexible Robot Arm: New Theoretical & Experimental Results. *IEEE Transactions on Automatic Control* 38(11): 1610-1622.
4. Wen Chen (2001) Dynamic Modeling of Multi-link Flexible Robotic Manipulators. *Computers & Structures* 79(2): 183-195.
5. V Feliu, JA Somolinos, A Garcia (2003) Inverse Dynamics based Control System for a Three Degrees-of-freedom Flexible Arms. *IEEE Transactions on Robotics & Automation* 19(6): 1007-1014.
6. V Feliu, F Ramos (2005) Strain Gauge based Control of Single-Link Flexible Very Light Weight Robots Robust to Payload Changes. *Mechatronics* 15(5): 547-571.
7. B Subudhi, AS Morris (2002) Dynamic Modeling, Simulation and Control of a Manipulator with Flexible Links & Joints. *Robotics and Autonomous Systems* 41(4): 257-270.
8. VG Moudgal, WA Kwong, KM Passino, S Yurkovich (1995) Fuzzy Learning Control for a Flexible-link Robot. *IEEE Transactions on Fuzzy Systems* 3(2): 199-210.
9. NC Singer, WC Seering (1990) Preshaping Command Inputs to Reduce System Vibration. *Journal of Dynamic Systems, Measurement & Control-Transactions of the ASME* 112: 76-82.
10. YP Chen, HT Hsu (2001) Regulation & Vibration Control of an FEM-based Single-link Flexible Arm using Sliding-mode Theory. *Journal of Vibration Control* 7(5): 741-752.
11. H Tjahyadi, K Sammut (2006) Multi-mode Vibration Control of a Flexible Cantilever Beam using Adaptive Resonant Control. *Smart Materials and Structures* 15: 270-278.
12. Juan R, Trapero Arenas, Mamadou Mboup, Emiliano Pereira Gonzalez, Vicente Feliu (2008) Online Frequency and Damping Estimation in a Single-Link Flexible Manipulator based on Algebraic Identification. *Proceedings of the 16th. Mediterranean Conference on Control & Automation (IEEE), Franco* pp: 338-343.
13. Emiliano Pereira, Summet Sunil Aphale, Vicente Feliu, SOR Moheimani (2011) Integral Resonant Control for Vibration Damping and Precise Tip-positioning of a Single-link Flexible Manipulator. *IEEE/ ASME Transactions on Mechatronics* 16(2): 232-240.
14. Jianhua Zhang, Ying Tian, Minglu Zhang (2014) Dynamic Model and Simulation of Flexible Manipulator based on Spring & Rigid Bodies. *Proceedings of the 2014 IEEE International Conference on Robotics & Biomimetics ('ROBIO-2014')* pp: 2460-2464.
15. J Feliu, V Feliu, C Cerrada (1999) Load Adaptive Control of Single-link Flexible Arms Based on a New Modeling Technique. *IEEE Transactions of Robotics & Automation* 15(5): 793-804.
16. RH Canon, E Schmitz (1984) Initial Experiments on the End-point Control of a Flexible Robot. *The International Journal of Robotics Research* 3(3): 62-75.
17. T Kotnick, S Yurkovich, U Ozguner (1998) Acceleration Feedback Control for a Flexible Manipulator Arm. *Journal of Robotic Systems* 5(3): 181-196.
18. Roy Debanik (2007) Estimation of Grip Force and Slip Behavior During Robotic Grasp Using Data Fusion and Hypothesis Testing: Case Study with a Matrix Sensor. *Journal of Intelligent and Robotic Systems* 50(1): 41-71.
19. Roy Debanik (2008) Stochastic Model-based Grasp Synthesis: New Logistics for Data Fusion with Dissimilar Sensor-cells. *Proceedings of the IEEE International Conference on Automation and Logistics (IEEE-ICAL 2008), Qingdao, China* 1-3: 256-261.
20. Roy Debanik (2018) Control of Inherent Vibration of Flexible Robotic Systems and Associated Dynamics. Springer Book. *Lecture Notes in Mechanical Engineering* pp: 201-222.

21. Warude P, Patel M, Pandit P, Patil V, Pawar H (2018) On the Design and Vibration Analysis of a Three-Link Flexible Robot Interfaced with a Mini-Gripper. Springer Book Lecture Notes in Mechanical Engineering pp: 29-46.
22. Roy Debanik (2020) Design, Modeling and Indigenous Firmware of Patient Assistance Flexible Robotic System-Type I: Beta Version. Advances in Robotics and Mechanical Engineering 2(3): 148-159.



This work is licensed under Creative Commons Attribution 4.0 License

To Submit Your Article Click Here: [Submit Article](#)

DOI: [10.32474/ARME.2022.03.000168](https://doi.org/10.32474/ARME.2022.03.000168)



### Advances in Robotics & Mechanical Engineering

#### Assets of Publishing with us

- Global archiving of articles
- Immediate, unrestricted online access
- Rigorous Peer Review Process
- Authors Retain Copyrights
- Unique DOI for all articles